PSFC/JA-07-20

Critical gradients and plasma flows in the edge plasma of Alcator C-Mod.

B. LaBombard[a], J.W. Hughes[a], N. Smick[a], A. Graf[b], K. Marr[a], R. McDermott[a], M. Reinke[a], M. Greenwald[a], B. Lipschultz[a], J.L. Terry[a], DG. Whyte[a], S.J. Zweben[c] and the Alcator C-Mod Team

December 2007

Plasma Science and Fusion Center
Massachusetts Institute of Technology
Cambridge MA 02139 USA

[a]*M.I.T. Plasma Science and Fusion Center - Cambridge, Massachusetts 02139*

[b]*University of California – Davis, California 95616*

[c]*Princeton Plasma Physics Laboratory – Princeton, New Jersey 08543*

This work was supported by the U.S. Department of Energy, Grant No. DE-FC02-99ER54512. Reproduction, translation, publication, use and disposal, in whole or in part, by or for the United States government is permitted.

Submitted for publication to *Physics of Plasma*.

Critical gradients and plasma flows in the edge plasma of Alcator C-Mod

B. LaBombard[*a], J.W. Hughes[a], N. Smick[a],
A. Graf[b], K. Marr[a], R. McDermott[a], M. Reinke[a],
M. Greenwald[a], B. Lipschultz[a], J.L. Terry[a],
D.G. Whyte[a], S.J. Zweben[c], and the Alcator C-Mod Team

[a]*MIT Plasma Science and Fusion Center, Cambridge, Massachusetts 02139*
[b]*University of California, Davis, California 95616*
[c]*Princeton Plasma Physics Laboratory, Princeton, New Jersey 08543*

Recent experiments have led to a fundamental shift in our view of edge transport physics: transport near the last-closed flux surface may be more appropriately described in terms of a critical gradient phenomenon rather than a diffusive and/or convective paradigm. Edge pressure gradients, normalized by the square of the poloidal magnetic field strength, appear invariant in plasmas with the same normalized collisionality, despite vastly different currents and magnetic fields – a behavior that connects with first-principles electromagnetic plasma turbulence simulations. Near-sonic scrape-off layer flows impose a co-current rotation boundary condition on the confined plasma when $B \times \nabla B$ points toward the active x-point, suggesting a link to the concomitant reduction in input power needed to attain high-confinement modes (H-mode). Indeed, L-mode plasmas are found to attain higher edge pressure gradients in this configuration, independent of the direction of B – evidence that SOL flows may affect transport and 'critical gradient' values in the edge plasma.

PACS: 52.30.-q, 52.25.Fi, 52.35.Ra, 52.40.Hf, 52.55.Fa, 52.70.Ds, 52.70.Nc

[*] Tel.: 1-617-253-7264, Fax: 1-617-253-0627: e-mail: labombard@psfc.mit.edu

I. INTRODUCTION

The performance of a fusion plasma depends largely on the transport phenomena in its edge region. This zone, which extends across closed magnetic field lines into the scrape-off layer (SOL), sets important 'boundary conditions' for the confined plasma: The height of the 'pedestal' formed in this region directly affects the overall energy confinement properties [1-5]; pedestal relaxation phenomena such as edge localized modes (ELMs [6]) and quasi-coherent oscillations [7,8] regulate the pedestal height, control core impurity content and, in the case of ELMs, can adversely impact divertor and first-wall components; intermittent, 'blobby transport' in the far SOL [9] enhances particle recycling on main-chamber walls [10] and is an integral part of tokamak density limit physics [11,12]; the width of the power exhaust channel is determined by cross-field transport in this zone and sets heat flux densities into the divertor; strong plasma flows in the SOL set a 'flow boundary condition' on the confined plasma, promoting co-current plasma rotation when $B \times \nabla B$ points toward the active x-point [13], and possibly accounting for the x-point dependence of the low-to-high confinement mode (L-H) power threshold [14]. Finally, the physics in this zone contains the secrets of the L-H transition itself.

Despite the importance of the edge plasma, there has been limited success in assembling physics-based prescriptions for the observed transport phenomenology. In particular, a quantitatively accurate, first-principles description that can reproduce both the observed time-averaged fluxes and profiles remains to be assembled – even for the 'simple' case when the plasma exhibits no ELM or quasi-coherent fluctuation phenomena. Nevertheless, significant progress has been made in recent years in understanding some fundamental aspects of the transport physics on both the experimental and theoretical/computational fronts.

On the experimental front, edge transport is found to be dominated by intermittent transport events, which span a full spectrum of frequency and magnitude (blobs and ELMs mentioned above). These observations tell us that a simple diffusive transport paradigm for the edge is woefully inadequate, even in the absence of ELMs. Instead, the transport phenomenology suggests a system near marginally stability, spawning intermittent transport events that are akin to 'avalanches' [15,16]. On the theoretical/computational front, significant progress has been made in assembling tools to perform first-principles 3-D electromagnetic plasma turbulence simulations [17], starting first with collisional Braginskii-like fluid models [18-20], progressing towards gyrofluid models [21,22], and generally heading towards gyrokinetic models [23-25].

While a quantitative match between simulation and experiment has yet to be demonstrated, experiments performed on Alcator C-Mod [26] have revealed clear connections between the operational space of the edge plasma (i.e., the attained densities, temperatures, pressure gradients) and dimensionless parameters that are known to 'control' the level of turbulence and transport in electromagnetic fluid drift turbulence (EMFDT) simulations. Two key dimensionless parameters are: (1) the local plasma pressure gradient normalized to the poloidal magnetic pressure, as parameterized by $\hat{\beta}$ in the work of Scott [18,27] and α_{MHD} in Rogers, Drake, Zeiler, *et al.* (RDZ) [19,28,29] and (2) the electron-ion plasma collision frequency normalized to characteristic turbulence time-scales, as parameterized by C_0 in Scott and α_d in RDZ. In particular, at fixed values of normalized collisionality, pressure gradients near the last-closed flux surface in L-mode discharges appear to be 'clamped' to a characteristic value of the MHD ballooning parameter (α_{MHD}), despite a wide variation in toroidal field and plasma current – a response suggestive of a system which is constrained by a 'critical pressure gradient'

condition. Peak pedestal pressure gradients in H-mode discharges are also found to yield fixed values of α_{MHD} for fixed collisionality over a wide variation in toroidal field, plasma current and gas fueling intensity, even in the absence of ELMs [30]. These observations point to a unified picture of edge plasma transport, rooted in the physics of electromagnetic plasma turbulence: independent of confinement mode and relaxation mechanism, pressure gradients near the last-closed flux surface tend to build toward a critical level, scaling with poloidal beta and influenced by collisionality; at or above this level, cross-field transport increases abruptly, either in the form of broadband turbulence or the onset of macroscopic relaxation mechanisms (i.e., ELMs, quasi-coherent oscillation, blobs) or both.

It should be noted that the idea of 'critical gradients' playing a role in edge transport is not new; it has been suggested both implicitly and explicitly in the work of others. For example, Hidalgo [31] has pointed out that the edge gradients behave in a way that suggests marginal stability; bursty transport events are more often observed when local gradients depart from the most-probable value. A critical poloidal beta-gradient (α_{MHD}) model was one of several possible candidates identified in early scaling studies of L-mode plasmas [32,33]. Pressure gradient e-folding lengths in the edge of H-modes on ASDEX Upgrade were found to scale as $L_{nTe} \sim n/I_p^2$ [34] with heat diffusivities scaling similarly [35] – observations that are largely consistent with α_{MHD} defining the operational boundaries of the discharge via pressure gradient driven instabilities [36]. As recounted by Neuhauser [37], the full range of edge plasma experiences on ASDEX and ASDEX Upgrade is entirely consistent with a critical-gradient transport paradigm, both for the behavior of the steep-gradient region near the separatrix and the rapid transport region in the far SOL.

As mentioned above, strong parallel flows are found in the SOL, which may be responsible for the x-point dependence of the H-mode power threshold. But, if this is true, might such flows also affect the pressure gradients attained in L-mode plasmas? Recent experiments in C-Mod indicate that SOL flows may indeed exert such influence; normalized L-mode pressure gradients (α_{MHD}) are found to be noticeably larger when the SOL flows promote co-current plasma rotation, i.e., when $B \times \nabla B$ points toward the active x-point [38,39].

This paper reviews and highlights key experimental observations that have led us to assemble the above picture of edge transport phenomenology – one of 'critical pressure gradients' set by the physics of EMFDT yet modified by the presence of edge plasma flows. Section II describes plasma diagnostics and discharges for the study. Ohmic L-mode discharges, in which scanning Langmuir-Mach probes can be used to interrogate edge conditions in detail, are the principal vehicle for this investigation. Measurements of plasma profiles and cross-field particle fluxes are presented in section III. Weak but persistent 'pedestals' are seen in L-mode discharges. As plasma density is raised, cross-field particle fluxes increase nonlinearly, yet density gradients do not change appreciably – basic evidence in support of a critical gradient transport paradigm. Connections between the observed edge conditions and the physics of EMFDT are made in section IV. Here we review the dimensionless parameters that 'control' EMFDT and examine experimental results, including new data from C-Mod, which support the hypothesis that such parameters are similarly operative in real edge plasmas. Section V turns to the subject of edge plasma flows, their dependence on magnetic topology and their apparent influence on the 'critical gradients' that are found in the near SOL. New measurements of scrape-off layer plasma flow profiles (both high-field and low-field sides) and charge-exchange

recombination spectroscopy measurements of toroidal flow just inside the separatrix of C-Mod are presented, highlighting the role that SOL flows play in setting a rotation boundary condition for the confined plasma. Data from discharges with forward and reversed magnetic field as well as upper and lower x-point topologies are found to support the notion that edge plasma flows impact the 'critical pressure gradients' found in the edge. Section VI summarizes the principal findings from these studies.

II. EXPERIMENTAL ARRANGEMENT

A cross-section of Alcator C-Mod [40] is shown in Fig. 1, with representative lower single-null (LSN) and upper single-null (USN) equilibria overlaid. High-resolution density and electron temperature profiles across the separatrix and scrape-off layer regions are assembled from edge Thomson scattering [41] plus inner and outer scanning Langmuir-Mach probes [42-44], which also record high resolution profiles of plasma flow along magnetic field lines. Recently, charge-exchange recombination spectroscopy (CXRS) diagnostics have been added for edge plasma flow measurements: Toroidal flow velocities of B^{+5} ions are inferred on the low-field side (~0 to ~35 mm inside separatrix) via CXRS, using a diagnostic neutral beam [45]; flow velocities of D^+ ions aligned with the local magnetic field (i.e., parallel flows) are inferred on the high-field side (~0 to ~12 mm inside separatrix) by looking at D_β charge-exchange recombination spectra, which is enhanced locally in response to a D_2 gas puff [46].

A toroidally-viewing Ly_α array (a new, advanced version of Ref. [47]) views the outer midplane of C-Mod (see Fig. 1). Combined with the measurements of plasma density, temperature and flows, these Ly_α measurements allow us to infer local ionization profiles and to perform simple particle balance analyses. In this way, particle fluxes across the separatrix and

SOL regions can be estimated and tracked systematically as plasma parameters are changed. Details of the analysis technique can be found in [10,11].

The behavior of edge plasma transport, profiles and flows has been studied over a wide range of plasma conditions, spanning several run campaigns. Figure 2 summarizes the different combinations of plasma current, I_p, and toroidal magnetic field, B_T, that have been covered, focusing here on ohmic L-mode discharges. Experiments during the 2000-2001 campaign concentrated on lower single-null discharges (LSN) with 'normal' directions of toroidal field and plasma current ($B \times \nabla B$ toward lower x-point, I_p aligned with B_T). More recent campaigns (2005-2007) have expanded the database to include upper single-null discharges (USN) with 'normal' field direction as well as LSN and USN with reversed field (i.e., $B \times \nabla B$ pointing up, I_p aligned with B_T). After the 2000-2001 run campaign, some changes to the scanning probe head geometries where made to improve their power handling and measurement capabilities, including a closer spacing of the electrodes and a change in the electrode orientation [44]. Recognizing that such changes might introduce a systematic bias in the different datasets (via differences in effective electrode collection area, for example), we have been careful not to mix probe data across campaigns; data from the 2000-2001 campaign are treated separately in the remainder of this paper. Line-averaged density ($\overline{n}_e$) scans were performed at each of the nominal combinations of (I_p, B_T), with a range of variation up to $0.1 < \overline{n}_e / n_G < 0.5$, where n_G is the empirical discharge density limit [48].

III. EDGE PLASMA PHEMONOLOGY: PROFILES AND FLUXES

A. SOL profiles

The response of edge plasma profiles to increased line-averaged density serves to illustrate some of the transport phenomenology. Figure 3 shows a series of composite density profiles assembled from Thomson and probe diagnostics. Plasma conditions are I_p = 0.78 MA and B_T = 5.2 tesla (ohmic L-mode), B_T = 3.3 tesla (ohmic EDA H-mode), or B_T = 3.0 tesla (ohmic ELM-free H-mode) with normal field direction in LSN. Similar to H-modes, a 'density pedestal' (albeit weak) is also seen in L-mode discharges. This steep gradient region near the separatrix in L-mode persists as $\overline{n}_e / n_G$ is raised via strong gas puffing, yet the far SOL tends to fill in systematically. For discharges with densities at or exceeding a level of $\overline{n}_e / n_G \sim 0.5$, the weak pedestal structure associated with the separatrix disappears – in fact the density near the separatrix starts to *decrease*; this condition corresponds to when electron temperatures *inside* the separatrix drop substantially [26] and to when the intermittent, 'bobby transport' (normally associated with the far SOL) starts to intrude onto closed magnetic field lines [11,49].

B. Flux-gradient relationships

While the above observations by themselves hint at an explosive growth of cross-field transport with increasing $\overline{n}_e / n_G$, we have the means of tracking cross-field particle fluxes directly. Using the midplane Ly_α array and detailed measurements of the SOL density and temperature profiles, the magnitude of particle flux densities across the SOL ($\Gamma_\perp$) can be estimated [10,11]. In essence, the technique exploits the tendency for the scrape-off layer fluxes in C-Mod to be dominated by 'main-chamber recycling', causing $\Gamma_\perp$ to be closely tied to the

ionization source profile in the main chamber. While the estimated particle flux densities are expected to be a factor of ~2 accurate at best, this technique allows $\Gamma_\perp$ to be tracked systematically as a function of discharge conditions.

The top panels in Fig. 4 shows density gradients and local $\Gamma_\perp$ as a function of line-averaged density, evaluated ~1 mm outside the last-closed flux surface. These discharges are from C-Mod's most recent run campaign (2007): $I_p = 0.8$ MA, $B_T = 5.4$ tesla with both 'normal' and 'reversed' field directions as well as upper and low-null topologies. The data have been binned according to line-averaged density with triangular symbols representing average values and vertical bars indicating ±1 standard deviation. Two key points are illustrated here: Cross-field particle flux densities in this steep density gradient region of the L-mode 'pedestal' grow nonlinearly with plasma density – a factor of ~20 for only a factor of ~4 increase in line-averaged density; despite the factor of ~20 increase in $\Gamma_\perp$, the local density gradient changes by only about a factor of ~2 ($B \times \nabla B$ pointing toward x-point) or not at all ($B \times \nabla B$ pointing away).

These observations warn us that a simple flux-gradient expression, $\Gamma_\perp \approx -D_{eff} \nabla_\perp n$, is a poor representation of the phenomenology; slight changes (or even no change) in $\nabla_\perp n$ are associated with large changes in $\Gamma_\perp$. The plots of particle flux density versus local density gradient in the bottom panel of Fig. 4 highlight this behavior; $\Gamma_\perp$ is clearly not a simple function of $|\nabla_\perp n|$. Perhaps $\Gamma_\perp$ is a strong non-linear function of $|\nabla_\perp n|$, but in this case it must also be a function of other hidden parameters in order to account for the non-monotonic dependence. More simply, the system behaves so as to keep $\nabla_\perp n$ in the steep gradient region *about the same* over a wide range of transport fluxes, i.e., the density gradient appears to be pinned to a 'critical gradient' condition. In this context, a diffusive (D_{eff}) or convective (V_{eff}) transport description

is of little value; such quantities must vary by large factors in order to account for the observed range in fluxes.

In view of the intermittent, 'blobby' transport phenomenon that is seen in the far SOL, the existence of a critical gradient condition in the near SOL is particularly appealing; such physics may be precisely what is needed to explain the overall transport dynamics. It is well established that fluctuations in the far SOL exhibit highly skewed probability distribution functions (PDFs) with 'algebraic tails', associated intermittency [15] and an overall dynamical behavior that is reminiscent of a self-organized critical system [50,51] (e.g., a 'sand pile'), exhibiting 'avalanche-like' transport phenomena (which correspond conceptually to the 'blobs' in the far SOL). Two principal ingredients are required for such a behavior: (1) a threshold condition, such as exceeding a critical gradient, which leads to the intermittent formation of plasma clumps and (2) a mechanism for rapid cross-field transport of the clumps. The mechanism for rapid radial transport in the far SOL is readily understood: curvature drift causes a dipole-like polarization of the clumps, resulting in an outward $E \times B$ motion. But, the near SOL may play the most important role – setting up a critical gradient threshold condition. It is interesting to note that an increased level of intermittency and long-time correlation has been detected in C-Mod's SOL fluctuations as the plasma density is systematically raised [52]. Yet, the dynamical origin of the fluctuation structures in the far SOL was not identified at that time. Perhaps as the density is raised and the plasma is 'pushed harder' against a critical gradient constraint in the near SOL, the system responds with both an explosive increase in the time-averaged fluxes and also a corresponding modification in the fluctuation dynamics.

Figure 4 also highlights another interesting phenomenon: Why should the value of the

'critical density gradient' care about $B \times \nabla B$ pointing toward or away from the x-point? Is this behavior somehow connected to the fact that the L-H power threshold is lower when $B \times \nabla B$ points toward the x-point? This question motivates the investigation of edge plasma flows in Sec. V.

IV. PHASE-SPACE OF THE NEAR SOL

A. Electromagnetic plasma turbulence – control parameters

A leading theoretical description of turbulence and transport in a collisional edge plasma can be broadly classified as low-frequency electromagnetic fluid drift turbulence (EMFDT), which has been the basis for a number or first-principles 3-D numerical simulations [18-20] (in particular, see recent review by Scott [17] and references therein). Because the edge plasma tends to reside in a collision-dominated regime (neoclassical collisionalities near the separatrix for the L-mode plasmas reported here are $\sim 10 < \nu^* < \sim 200$), a fluid description is often justified; the starting point for these models has therefore been a set of Braginskii-like plasma fluid equations [53], coupled with an electromagnetic model that accounts for finite inductance in parallel Ohm's law and handles the associated magnetic field perturbations.

Initial work by Scott [18,27] and Rogers, Drake, Zeiler, *et al.* (RDZ) [19,28,29] explored and identified the principal dimensionless parameters that govern the plasma dynamics and control magnitude of turbulence and resultant cross-field transport. These are: (1) local plasma pressure gradient normalized to the poloidal magnetic pressure (parameterized by $\hat{\beta}$ in the work of Scott and α_{MHD} in RDZ) and (2) the electron-ion plasma collision frequency normalized to characteristic turbulence time-scales (parameterized by C_0 in Scott and α_d in RDZ – see Table 1 in Ref. [26] for relationships). Heat and particle diffusivities are found to be strong, non-linear

functions of both beta gradient (α_{MHD} or $\hat{\beta}$) and collisionality parameter (α_d or C_0) in some regimes. For example, a regime of very large cross-field transport at high collisionality and low beta gradient was identified by RDZ [19] and associated with the onset of a transport-defined tokamak density limit; the underlying dynamics has since been explored in more detail by Guzdar [54]. Later, Xu and coworkers used the electromagnetic fluid turbulence code BOUT [55] (which models the magnetic x-point geometry) to study the transport behavior as the empirical density limit is approached [56]; simulations were found to qualitatively reproduce a 'density-limit' behavior as originally identified by RDZ: a rapid increase in cross-field transport was recorded as density was raised (α_d decreased) or plasma current reduced (α_{MHD} increased) – a behavior that makes contact with the data shown in Fig. 4 and discussed further in Ref. [26]. In addition, due to electromagnetic effects in these models, cross-field transport was found to increase strongly with beta gradient, well before the onset of the ideal MHD limit ($\alpha_{MHD} \sim 1$) [18,29]. Most notably, Scott used the electromagnetic fluid turbulence code, DALFTI, to systematically examine the transport scaling with α_{MHD} in moderate collisionality plasmas [57]; an explosive growth in cross-field transport was found when α_{MHD} exceeded the critical value of $\alpha_{MHD\,crit} \sim 0.2$, a point where the mode structure transitions from drift wave to ideal ballooning (see Figs. 23-25 in Ref. [57]).

B. Edge plasma phase space

Inspired and guided by these theory/modeling developments, we began to explore plasma conditions near the separatrix in Alcator C-Mod in terms of the 'phase-space' that defines EMFDT, namely, normalized pressure gradient and collisionality [26]. (Magnetic shear is also known to be an important parameter [58], but has not been a significant variable for the magnetic

topologies investigated up to now.) A key result of this initial investigation (2000-2001 campaign) is reproduced in Fig. 5. – normalized pressure gradients, α_{MHD}, measured at a location 2 mm outside the separatrix are plotted versus an inverse collisionality parameter, $\Lambda \equiv \left(\lambda_{ei}/R\right)^{1/2}/q_{95}$. Here, λ_{ei} is the local electron-ion mean free path, R is major radius and q_{95} is the rotational transform at the 95% flux surface. The form of this 'inverse collisionality parameter', Λ, is chosen to have the same λ_{ei} and q_{95} dependences in the 'diamagnetic parameter', α_d, of RDZ ($\Lambda \sim \alpha_d \left(L_n/R\right)^{1/4}$) and the collisionality parameter, C_0, of Scott ($\Lambda \sim C_0^{-1/2}\left(R/L_{pe}\right)^{1/2}$). Yet, Λ is free of embedded density (L_n) or electron pressure (L_{pe}) gradient scale-length normalizations. In this way all the gradient information in the two-parameter 'phase-space', (α_{MHD}- Λ), is contained in the single parameter, α_{MHD}.

The data in Fig. 5 exhibit an number of remarkable features: (1) Despite the significant variation in plasma current (factor of ~2) and magnetic field (factor of ~1.5), the 'edge plasma state' near the separatrix is found to remain roughly invariant, i.e., similar values of α_{MHD} are obtained when the local value of Λ is the same, (2) these invariant values of α_{MHD} are in the range where transport is thought to grow rapidly with α_{MHD}, $\alpha_{MHD} > \alpha_{MHD\,crit} \sim 0.2$ [57], (3) for values of $\Lambda <$ ~0.25, normalized pressure gradients fall with decreasing Λ (i.e., increasing plasma density). The latter point connects with the results in Figs. 3 and 4 and the 'density limit' behavior discussed above – owing to a rapid increase in cross-field transport, the region of high pressure gradient at high collisionality is largely inaccessible to experiments.

Data from C-Mod's more recent run campaigns (Fig. 6) have tested and verified the above relationships over a wider variation in plasma current (factor of ~2.7), magnetic field

(factor of ~2) as well as with different x-point topologies. Absolute and normalized pressure gradients measured at a distance 1 mm outside the separatrix are shown for LSN and USN topologies with normal field direction. Independent of magnetic topology, electron pressure gradients are seen to trace out distinct families of curves that depend on plasma current. Yet, when normalized by plasma current squared ($\alpha_{MHD} \propto |\nabla n T_e| / I_p^2$) the data points for a given topology are found to overlay. [Note: Small quantitative differences are evident between the 'phase-space' mappings of Figs. 5 and 6. Probe diagnostic modifications and/or systematic variations in flux-surface mappings between the 2000-2001 and later run campaigns are thought to be the cause.]

The persistent scaling of pressure gradients with I_p^2 (Figs. 5 and 6) constitutes strong evidence that α_{MHD} is indeed a dimensionless 'control parameter' for the underlying edge transport physics. Moreover, the clustering of edge plasma states into such a narrow band suggests that local pressure gradients are being clamped by a 'critical value' of α_{MHD} (i.e., a value of α_{MHD} beyond which the transport grows rapidly). In this sense, $\alpha_{MHD\,crit}$ also appears to be a function of collisionality. But, what evidence do we have that the EMFDT-inspired parameter, Λ, is a 'correct' collisionality parameter for the horizontal axis of this phase-space? Figure 7 explores two alternative phase-spaces for the LSN data in Fig. 6: one where the inverse collisionality axis is replaced by $(\lambda_{ei}/R)^{1/2}$ and another where it is replaced by $(\lambda_{ei}/q_{95}R)^{1/2} \sim 1/\nu^{*1/2}$. The latter normalization is of interest since ν^* is the neoclassical collisionality parameter. Based on the clustering of the data points in Fig. 7, we conclude that the dimensionless grouping of $(\lambda_{ei}/R)^{1/2}/q_{95}$ is indeed superior to the other two. The strong q_{95}

dependence in Λ is just what is needed to align the data from different plasma currents. In this regard, the EMFDT-inspired control parameter, Λ, does indeed appear to be an appropriate dimensionless parameter for the horizontal axis of this phase-space; by comparison, neoclassical collisionality ($1/\nu^{*1/2}$) does not.

Returning to Fig. 6, we see another interesting trend: LSN plasmas ($B \times \nabla B$ toward the x-point) appear to attain higher values of α_{MHD} compared to USN topology ($B \times \nabla B$ away) – a result similar to that noted for $\nabla_{\perp} n$ in Fig. 4. In search for a potential explanation for this behavior, we now turn to the subject of edge plasma flows.

V. EDGE PLASMA FLOWS

A. Magnetic topology effects

Experiments in Alcator C-Mod have uncovered clear connections between magnetic x-point topology (LSN/USN) and edge plasma flows [13]. The top panels of Fig. 8 show representative plasma flows in both the high- and low-field side scrape-off layers, measured by Langmuir-Mach probes. Also shown in Fig. 8 are toroidal flow velocity measurements from recently installed CXRS diagnostics. These data were taken from a series of matched discharges, covering the four permutations of LSN/USN and normal/reversed field (I_p = 0.8 MA, B_T = 5.4 tesla, $\overline{n}_e / n_G$ = 0.27). The drawings in the bottom panels of Fig. 8 illustrate the topologies and field directions. The dominant parallel flow directions in the SOL are also indicated (poloidal projections are shown).

According to the evidence presented in Ref. [13], ballooning-like cross-field transport asymmetries cause excess plasma to appear in the low-field SOL; the resultant pressure imbalance drives strong parallel plasma flows, which encircle the confined plasma (see bottom

panels of Fig. 8). Resultant flows in the high-field side SOL can approach the local sound speed (for reference, D^+ sound speed is ~50 km s^{-1} at 25 eV) and are co-current directed when $B \times \nabla B$ points toward the active x-point. (Henceforth we designate this direction as 'favorable $B \times \nabla B$'.) As discussed in Ref. [13], these 'transport-driven flows' impose a toroidal rotation boundary condition on the confined plasma, which under certain conditions causes the plasma to 'spin up' in the co-current direction for favorable $B \times \nabla B$. The new CXRS measurements in Fig. 8 independently verify this picture. The largest flow velocities in the system reside in the high-field SOL; plasma velocity inside the separatrix is seen to change toroidal direction as flows in the high-field side SOL change direction. In contrast, parallel flows in the low-field SOL are persistently co-current directed, yet these are modulated towards a stronger/weaker co-current flow in response to $B \times \nabla B$ being favorable/unfavorable. This behavior is consistent with such flows being primarily the sum of a Pfirsch-Schluter component (persistently co-current directed) plus a toroidal rotation component (with direction dependent on $B \times \nabla B$) [13].

As the plasma density is varied, the confined plasma's toroidal rotation appears to respond differently to the transport-driven SOL flows (see Fig. 9). The large flow velocities in the high-field SOL remain strong over the full density variation; their co/counter direction is set by favorable/unfavorable $B \times \nabla B$. Weaker toroidal velocities just inside the separatrix on the high-field side also show a persistent dependence on $B \times \nabla B$, with some hint of a reduced $B \times \nabla B$ dependence at low density. In contrast, toroidal velocities inside the separatrix on the low-field side vary with plasma density and become offset to a co-current velocity that is insensitive to $B \times \nabla B$ at the lowest densities. [Note: The LSN, normal-field data at low density are suspect here. By symmetry arguments, these should overlay with the USN reversed field

data, but they do not – we have not yet identified a reason for this behavior.] Parallel flows in the low-field SOL tend to mimic the response of toroidal flows inside the separatrix; their sensitivity to favorable/unfavorable $B \times \nabla B$ is absent at the lowest densities.

The data in Figs. 8 and 9 tell us that edge flows and plasma rotation are fundamentally different in L-mode plasmas with favorable versus unfavorable $B \times \nabla B$; depending on plasma density, the confined plasma tends to 'spin-up' in respective co- or counter-current directions. Langmuir probe data independently support this picture, reporting different radial electric fields in the SOL in LSN versus USN discharges (normal field direction), with values that are roughly consistent with the inferred change in toroidal rotation [13]. This interesting link between plasma flow/rotation and magnetic topology has been suggested as an explanation for the ubiquitous x-point dependence of the L-H power threshold in tokamaks [14], which is lower for favorable $B \times \nabla B$. Presumably, the underlying physics involves differences in equilibrium $E \times B$ flow shear in the vicinity of the separatrix, a quantity that we do not presently measure in C-Mod. Nevertheless, the observed correlations among SOL flow, toroidal rotation, L-H threshold, and favorable/unfavorable $B \times \nabla B$ are quite robust and compelling [14]. Can such differences in plasma flow/rotation also explain the observed $B \times \nabla B$ dependence of the flux/gradient relationships (Fig. 4) and 'critical pressure gradients' (Fig. 6) in C-Mod'?

B. Connection between plasma flows and gradients

The top panels in Fig. 10 show the familiar phase-space plots of normalized edge pressure gradient (α_{MHD}) versus inverse collisionality parameter (Λ) for the same set of discharges examined in Fig. 9. The trend of higher α_{MHD} with favorable $B \times \nabla B$ that was initially seen in Fig. 6 is verified here for both forward and reversed magnetic field directions

(differences are highlighted in yellow). These data reassure us that the differences in edge pressure gradients are truly associated with favorable/unfavorable $B \times \nabla B$ and are not the result of some diagnostic artifact and/or subtleties arising from the different upper and lower divertor geometries in C-Mod (see Fig. 1). Also plotted in the bottom panels of Fig. 10 are the corresponding parallel flow measurements in the low-field side SOL. As discussed above, these flows are sensitive to favorable/unfavorable $B \times \nabla B$, reflecting the trend of the confined plasma to rotate in the corresponding co- or counter-current directions, with magnitude dependent on plasma density (or more generally, collisionality).

Finally, the plots in Fig. 10 reveal a correlation between pressure gradients and flows. In the range of moderate-to-high collisionality ($\Lambda < \sim 0.3$), significantly higher values of α_{MHD} are attained for favorable $B \times \nabla B$. Coincidently, over roughly the same collisionality range, plasma flows in the low-field SOL are enhanced towards the co-current direction. Thus, not only are edge flows/rotation fundamentally different in these L-mode plasmas (i.e., dependent on $B \times \nabla B$), normalized pressure gradients near the separatrix are also fundamentally different, with a clear correlation exhibited between the two. In low collisionality ranges (high Λ) where favorable $B \times \nabla B$ does not lead to a positive increment in co-current plasma rotation, no corresponding enhancement in α_{MHD} is seen. [Note: The insensitivity of confined plasma rotation to $B \times \nabla B$ direction (and corresponding direction of high-field side SOL flows) at low collisionality is by itself an interesting observation – a phenomenon that we do not yet understand.]

While the above observations certainly do not prove a causal relationship between edge flows/rotation and gradients, they constitute strong circumstantial evidence. Such observations

resonant with the idea that the x-point dependence of the L-H power threshold (and its associated differences in edge electron temperature or temperature gradient 'threshold' [59,60]) involves edge flows and plasma rotation [14]: L-mode discharges with favorable $B \times \nabla B$ tend to have 'favorable' co-current toroidal rotation; when this happens, these discharges attain higher edge pressure gradients – discharges that also require the least amount of auxiliary power to attain the H-mode confinement regime.

Since a leading explanation for the L-H transition (and for turbulence suppression in general) involves $E \times B$ velocity shear [61-65], this physics should also connect the observed differences in edge plasma flow/rotation behavior (affected by favorable/unfavorable $B \times \nabla B$) to the corresponding differences in the 'critical gradients' that we observe. This is an area that is ripe for investigation, which we hope to report on in future publications.

VI. SUMMARY

The edge plasma in a tokamak (L or H-mode) is marked by a persistent, steep-gradient region near the last-closed flux surface. This region, which forms the 'pedestal' of an H-mode plasma, supports a rich variety of phenomenology that transports particles and energy into and across the scrape-off layer: ELMs, quasi-coherent oscillations, intermittent blobby transport. Yet, gradients in this region are observed to be remarkably 'stiff' – peak pressure gradients in C-Mod's H-mode pedestals are found to scale with plasma current squared, regardless of being in ELM-free, ELMy, or quasi-coherent mode dominated (EDA H-mode) regimes [30]. L-mode density gradients at the last-closed flux surface also exhibit stiffness: a factor of ~20 increase in cross-field particle fluxes cases local density gradients to change by only a factor of ~2 or not at all, depending on $B \times \nabla B$ relative to the active x-point. These data highlight two important

aspects of edge transport phenomenology: (1) Simple flux-gradient expressions, $\Gamma_\perp \approx -D_{eff}\nabla_\perp n$, are a poor representation of the time-averaged edge transport; instead, the system appears to be observing a 'critical gradient', clamping the density gradient to a narrow parameter range, $\nabla_\perp n \sim \nabla_{\perp crit} n$; (2) yet, despite their insensitivity to the transport fluxes, edge gradients are remarkably sensitive to magnetic x-point topology – an observation reminiscent of the L-H power threshold, its magnetic topology dependence and the correspondingly different edge flow and plasma rotation conditions that have been correlated with it [14].

These and other observations on C-Mod [26], have contributed to our present view of edge transport physics – one of 'critical pressure gradients' set by the physics of electromagnetic plasma turbulence yet modified by the presence of edge plasma flows. Over a range of plasma currents and magnetic fields, pressure gradients near the separatrix in ohmic L-mode plasmas are found to scale with plasma current squared when the local value of normalized collisionality is held fixed – a behavior that is broadly consistent with what one might expect from electromagnetic fluid drift turbulence (EMFDT) [17-19,29,57], which among other things identifies poloidal beta gradient ($\alpha_{MHD} \propto |\nabla n T_e| / I_p^2$) and collisionality ($\sim 1/\Lambda$) as controlling dimensionless parameters. When mapped to this two-parameter 'phase-space', (α_{MHD}-Λ), the edge plasma state in Alcator C-Mod is found to be largely invariant – strong evidence that EMFDT controls the edge state.

Encouraged by initial studies [26], we have since performed more rigorous tests of the 'critical pressure gradient' behavior and its mapping onto the two-dimensional 'phase-space', (α_{MHD}-Λ); plasmas with an expanded range of currents, magnetic fields, forward and reversed magnetic field direction and upper/lower-null magnetic topologies (USN/LSN) have now been

explored. The relationships uncovered in the earlier work are found to be quite robust: edge plasma states remain invariant when mapped to (α_{MHD}-Λ) space, over the full range of plasma conditions studied thus far. Poloidal beta gradient, α_{MHD} and the inverse collisionality parameter, $\Lambda = (\lambda_{ei}/R)^{1/2}/q_{95}$, appear to contain the relevant dimensionless groupings. When mapped to a phase-space that defines inverse collisionality according to mean-free path over machine size, $(\lambda_{ei}/R)^{1/2}$, or inverse neoclassical collisionality, $(\lambda_{ei}/q_{95}R)^{1/2} \sim 1/\nu^{*1/2}$, edge plasma states are found to vary with q_{95}; when mapped to (α_{MHD}-Λ) space, they do not. However, magnetic x-point topology is found to somehow influence the mapping – higher normalized pressure gradients are obtained in L-mode plasmas for 'favorable $B \times \nabla B$', i.e., when $B \times \nabla B$ points toward the active x-point.

Differences in edge plasma flows and toroidal plasma rotation are examined as a possible explanation for the $B \times \nabla B$ dependence. New data from Langmuir-Mach probes combined with CXRS measurements inside the separatrix have been used to track SOL flows and toroidal plasma rotation in ohmic L-mode plasmas. The picture originally presented in Ref. [13] has been independently verified: 'transport-driven' SOL flows impose an x-point dependent, co-current or counter-current 'flow boundary condition' on the confined plasma, according to favorable versus unfavorable $B \times \nabla B$ direction; the confined plasma responds to the SOL flows, rotating in the respective co-current or counter-current directions. Plasma density (collisionality) is found to influence the plasma rotation, with low density plasmas ($\overline{n}_e / n_G$ < ~ 0.2) exhibiting a diminished sensitivity to $B \times \nabla B$ direction.

A clear correlation is found between the $B \times \nabla B$ dependence of SOL flows/rotation and

differences in the phase-space mappings: in the range of collisionalities where α_{MHD} is enhanced by favorable $B \times \nabla B$, significantly higher co-current parallel flows are observed in the low-field side SOL; co-current rotation of the confined plasma is correspondingly higher. This observation makes direct contact with the L-H power threshold being lower for favorable $B \times \nabla B$ – edge plasma flows/rotation and edge pressure gradients are fundamentally different; plasmas with favorable $B \times \nabla B$ naturally attain higher pressure gradients; these require less auxiliary power to attain H-mode.

While the data presented in this paper certainly do not prove causal relationships between edge flows/rotation and 'critical gradients', they represent strong evidence in support of this dynamic. Further experiments are clearly needed to test these inferences and to expose more of the underlying physics – in particular a systematic examination of $E \times B$ velocity shear profiles across the LCFS; we hope that our observations reported here will help motivate such studies.

The connections drawn here between edge pressure gradients scalings in C-Mod and the dimensionless parameters of electromagnetic plasma turbulence simulations are encouraging – a strong endorsement of this theoretical framework. Yet, the details remain a challenge for future simulation work: Much of the edge plasma phenomenology described in this paper – including the formation of the steep 'critical gradient' region near the separatrix and the magnitude of the observed transport fluxes – remain to be accurately reproduced by any first-principles numerical simulation.

Acknowledgements

Alcator C-Mod's contributions to fusion energy science are made possible by the excellent engineers, technical staff, students, and scientists on the Alcator team. This work is supported by U.S. Department of Energy Coop. Agreement DE-FC02-99ER54512.

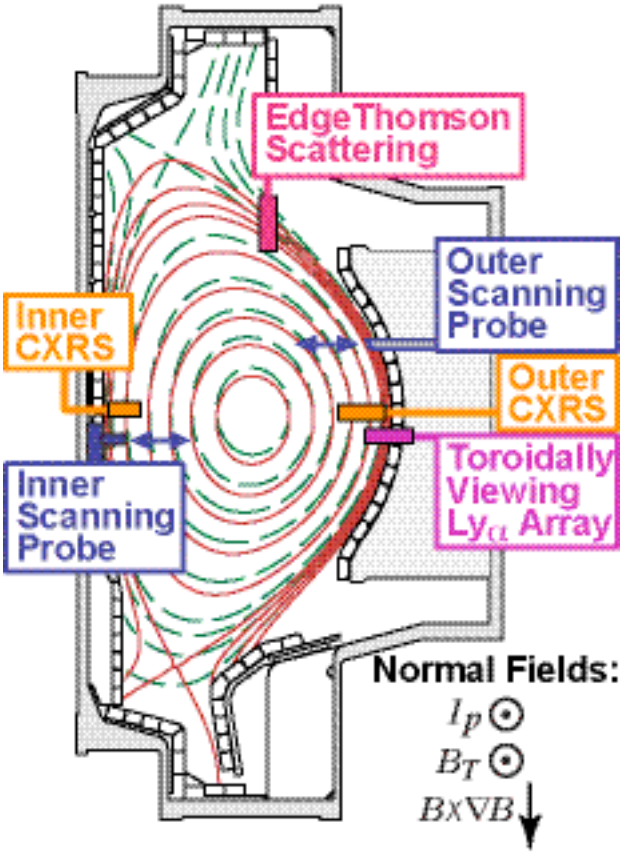

FIG. 1. (Color online) Cross-section of Alcator C-Mod with representative lower-null (solid lines) and upper null (dashed lines) equilibria overlaid. Scanning probe, Thomson scattering and charge-exchange recombination spectroscopy (CXRS) diagnostics record a composite picture of plasma profiles and flows across the separatrix and into the SOL on the high- and low-field sides. Plasma fluxes in the low-field SOL are estimated from a particle balance technique [10], using ionization profiles inferred from a toroidally-viewing Ly$_\alpha$ diagnostic.

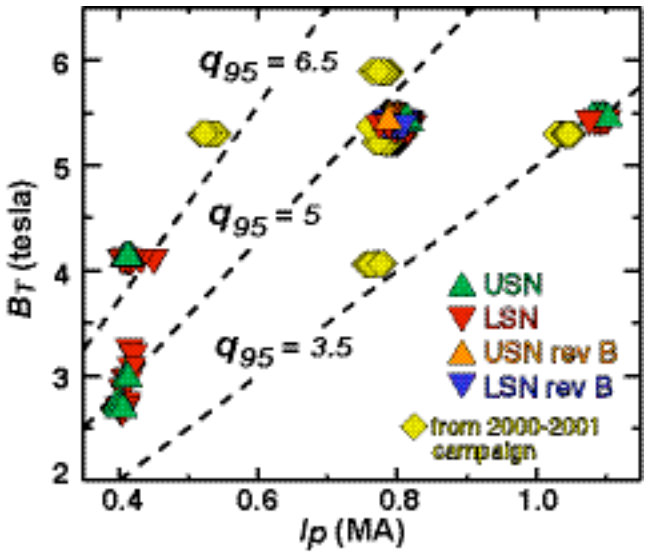

FIG. 2. (Color) Toroidal magnetic fields (B_T) and plasma currents (I_p) for ohmic L-mode discharges investigated across different run campaigns. Results are reported in this paper that extend the 2000-2001 dataset to lower values of B_T and I_p, allowing more stringent tests of the conclusions reported in Ref. [26]. In addition, the influences of x-point location (LSN/USN) and magnetic field direction have now been explored.

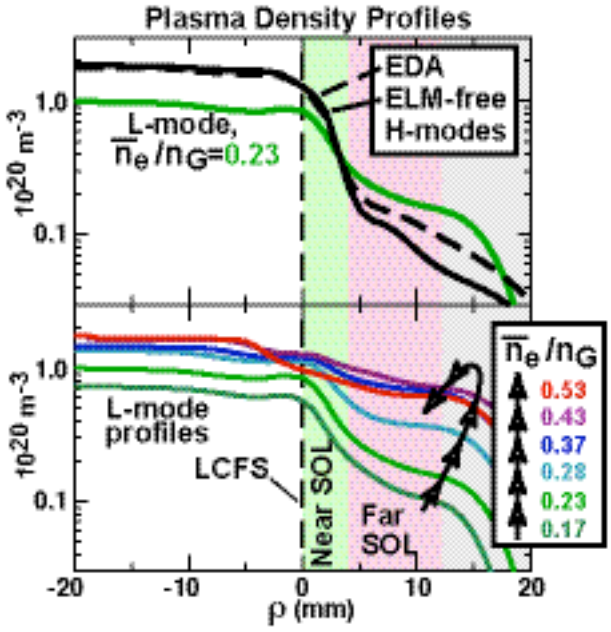

FIG. 3. (Color) Composite density profiles assembled from probe and Thomson diagnostics for both ohmic L-mode and H-mode discharges. A persistent, steep density gradient 'pedestal' is seen in the near SOL of both L and H-mode discharges. As line-averaged density is increased, plasma 'fills in' the far SOL. (Note: although much of the H-mode 'density pedestal' is seen to occur in the near SOL in these ohmic discharges, the electron temperature pedestal forms inside the LCFS causing the steepest pressure gradients to form there, as can be seen in Fig. 7 of Ref. [26].)

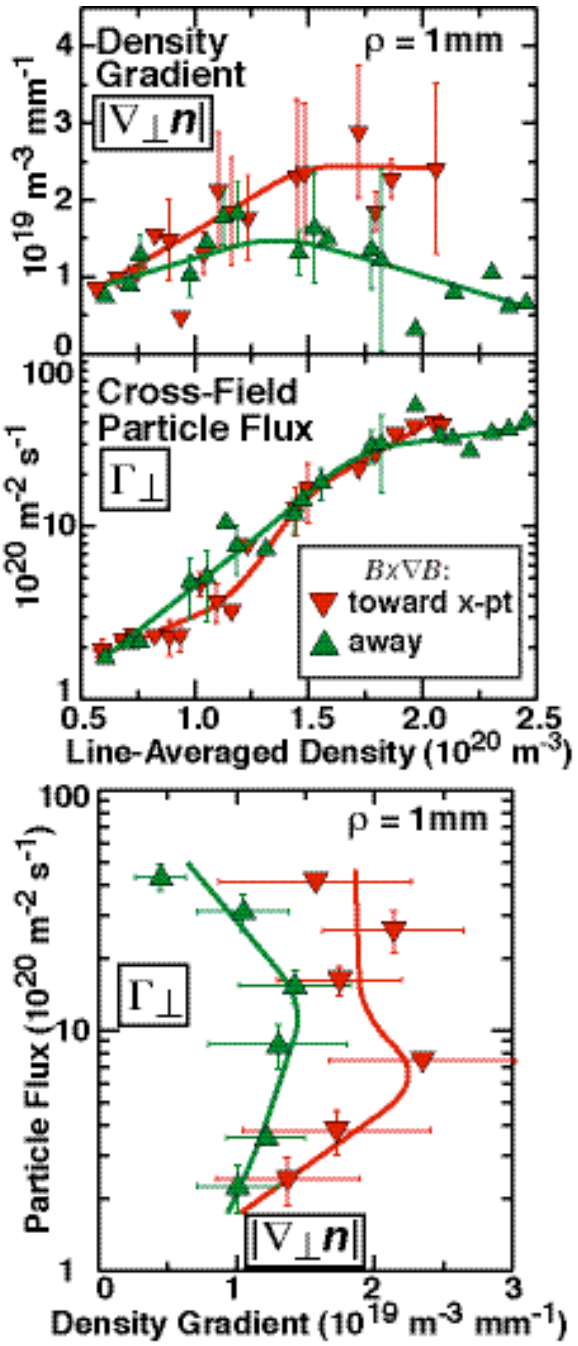

FIG. 4. (Color online) Plasma density gradient and cross-field particle flux densities at a location ~1 mm outside the separatrix versus line averaged-density (top) and versus each other (bottom). Data are included from LSN and USN topologies with both normal and reversed magnetic fields. A factor of ~20 increase in particle flux is associated with a factor of ~4 increase in line density. Yet, local density gradients increase by only a factor of ~2 or even not at all, depending on the direction of $B \times \nabla B$. The resultant flux-gradient relationships (bottom panel) highlight the insensitivity of local flux to gradient value. Over the full range of fluxes, density gradients appear to be clamped near a 'critical gradient' that depends on the direction of $B \times \nabla B$.

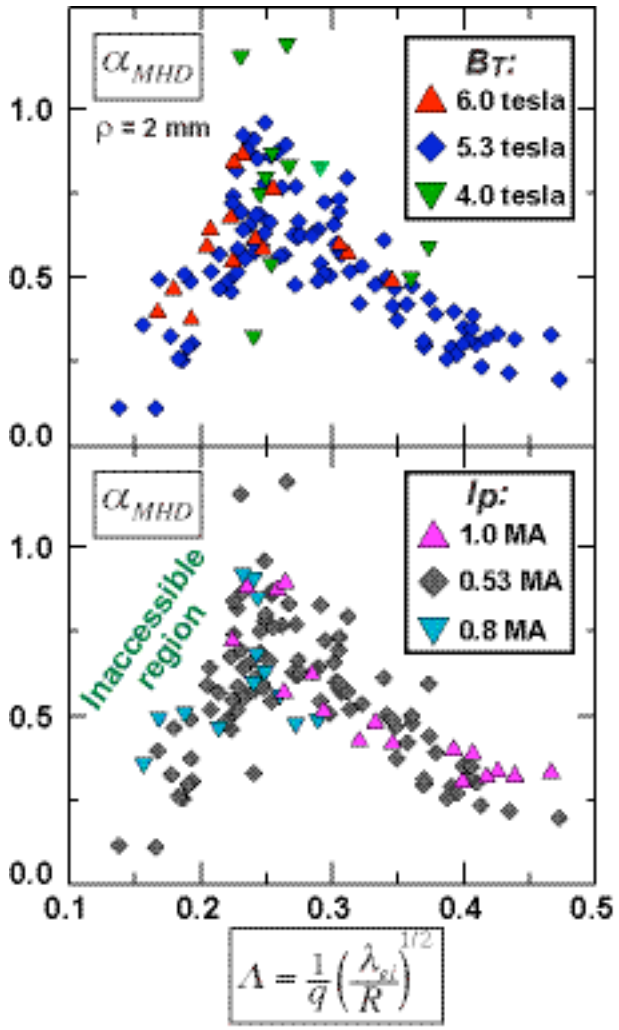

FIG. 5. (Color online) Normalized pressure gradients, α_{MHD}, at a location 2 mm outside the separatrix are plotted versus inverse collisionality parameter, Λ. The edge plasma state is found to map to a well-defined band in this two parameter phase-space, despite significant variation in plasma current (I_p) and magnetic field (B_T). Discharges are from the 2000-2001 campaign, shown in Fig. 2.

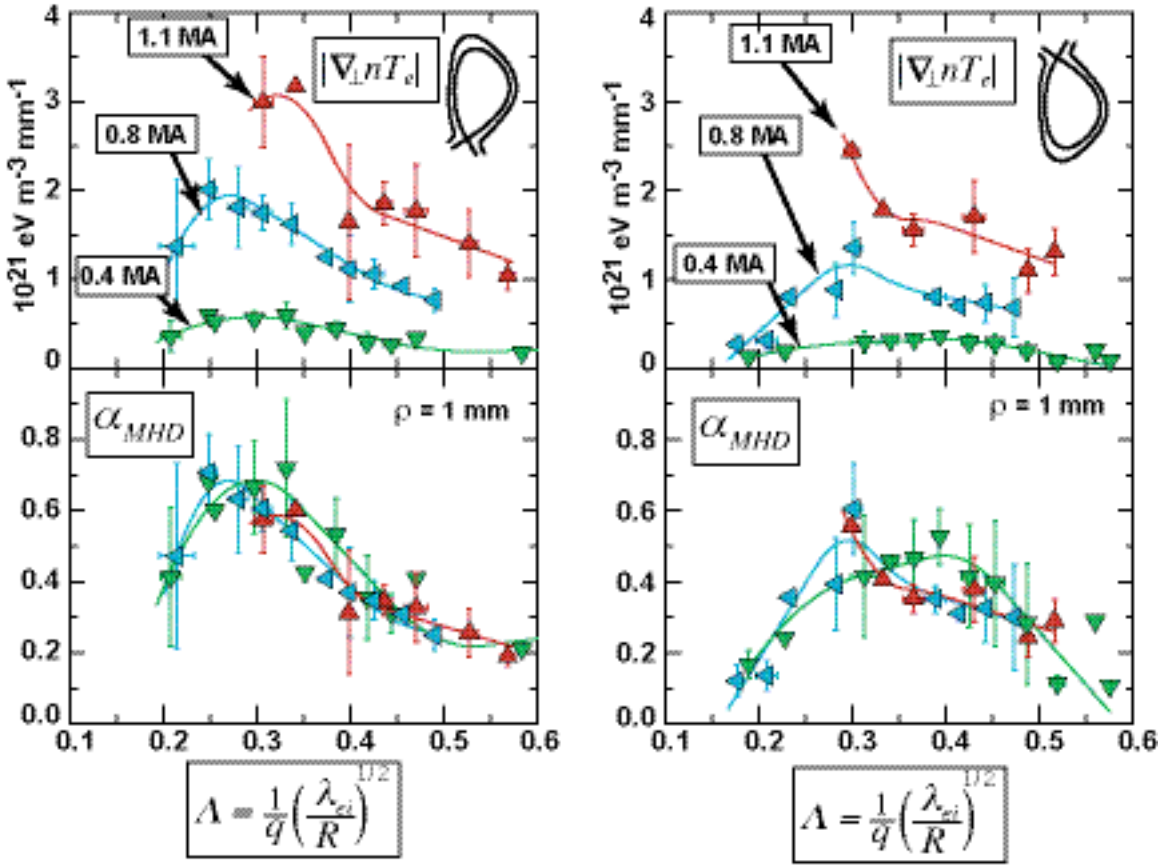

FIG. 6. (Color online) Electron pressure gradients and α_{MHD} versus Λ evaluated 1 mm outside the separatrix in LSN discharges (left) and USN discharges (right) with normal magnetic field direction. Data points represent average values from a number of probe scans; error bars indicate typical ±1 standard deviation in data sample; smooth curves are spline fits to the data.

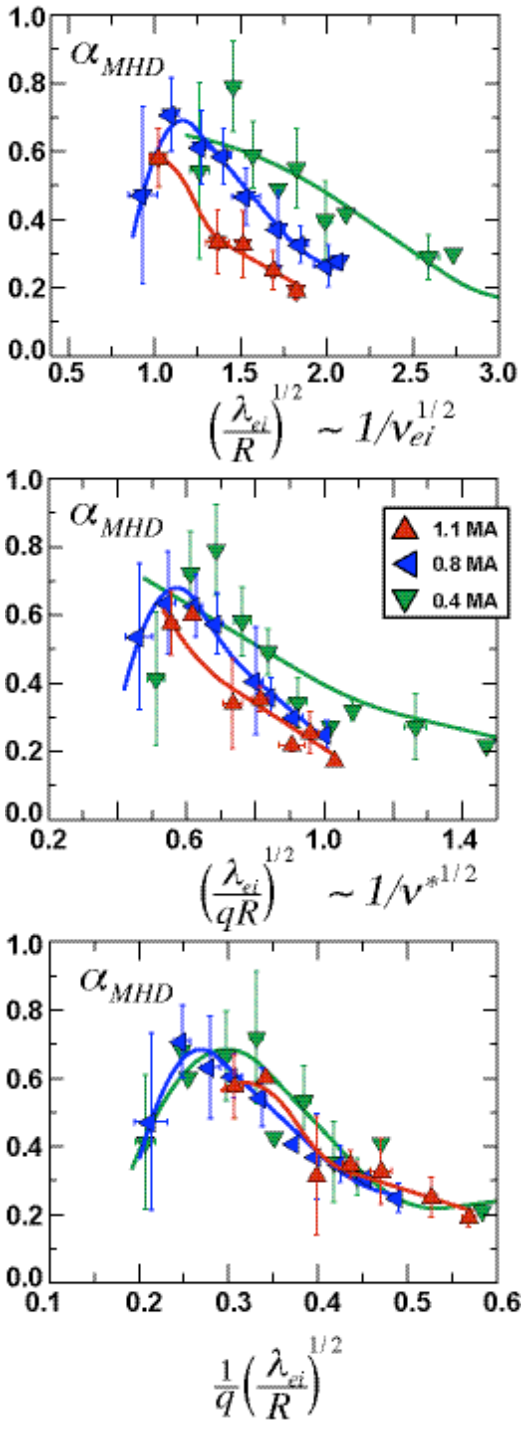

FIG. 7. (Color online) α_{MHD} values from LSN discharges in Fig. 6 plotted versus three different inverse collisionality normalizations.

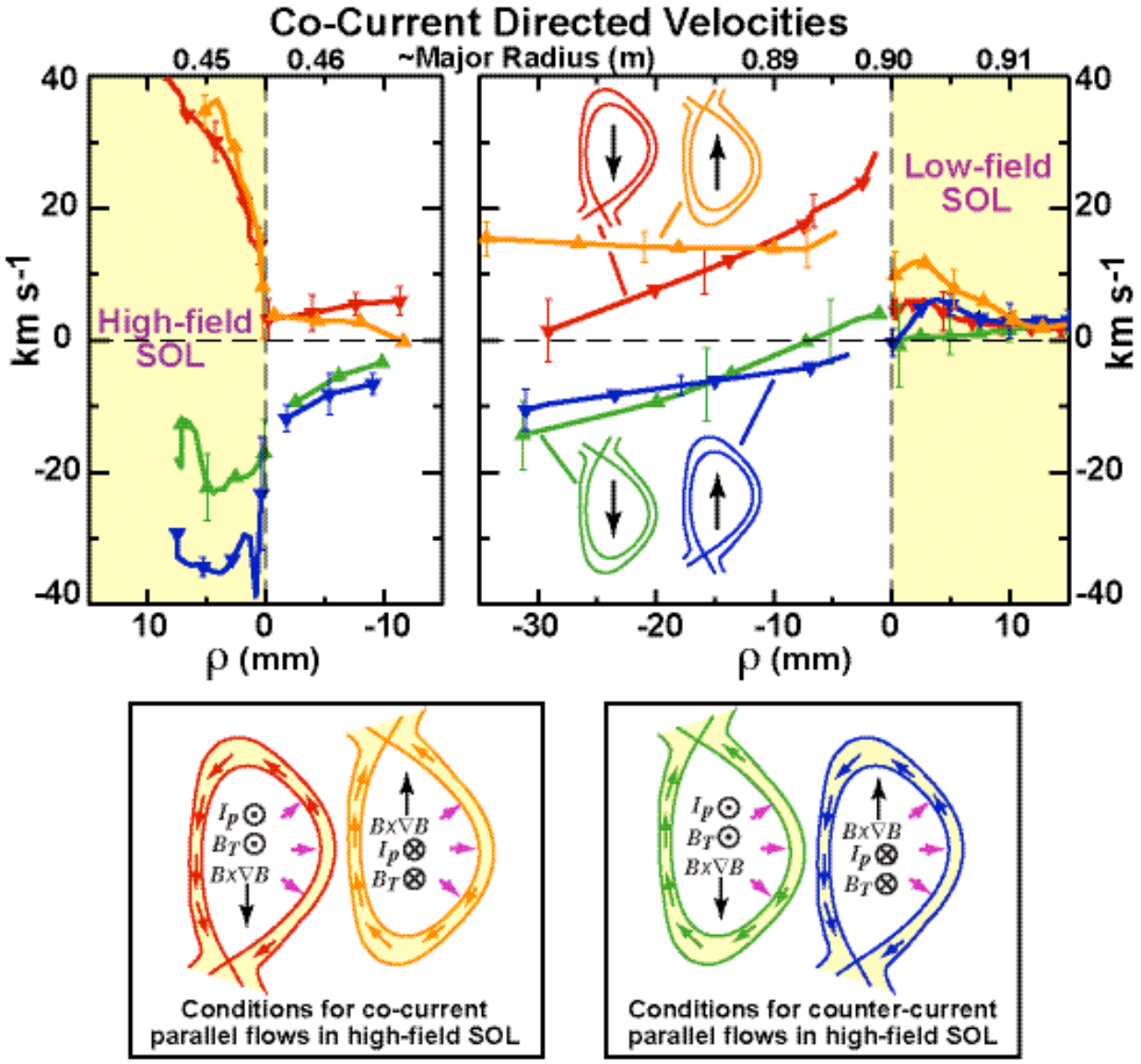

FIG. 8. (Color) Top panels – a composite picture of plasma flow profiles assembled from Langmuir-Mach probes (parallel flow velocities in the high- and low-field SOL regions) and CXRS diagnostics (toroidal velocities of B^{+5} on the low-field side and parallel velocities of D^{+} on the high-field side, both inside the separatrix). ρ is a flux-surface label corresponding to the distance outside the separatrix, mapped to the outer midplane; positive velocities indicate flow towards the co-current direction. Bottom panels – cartoon drawings of x-point topologies, field directions and poloidal projections of the prominent parallel flows that are measured in the high-field SOL.

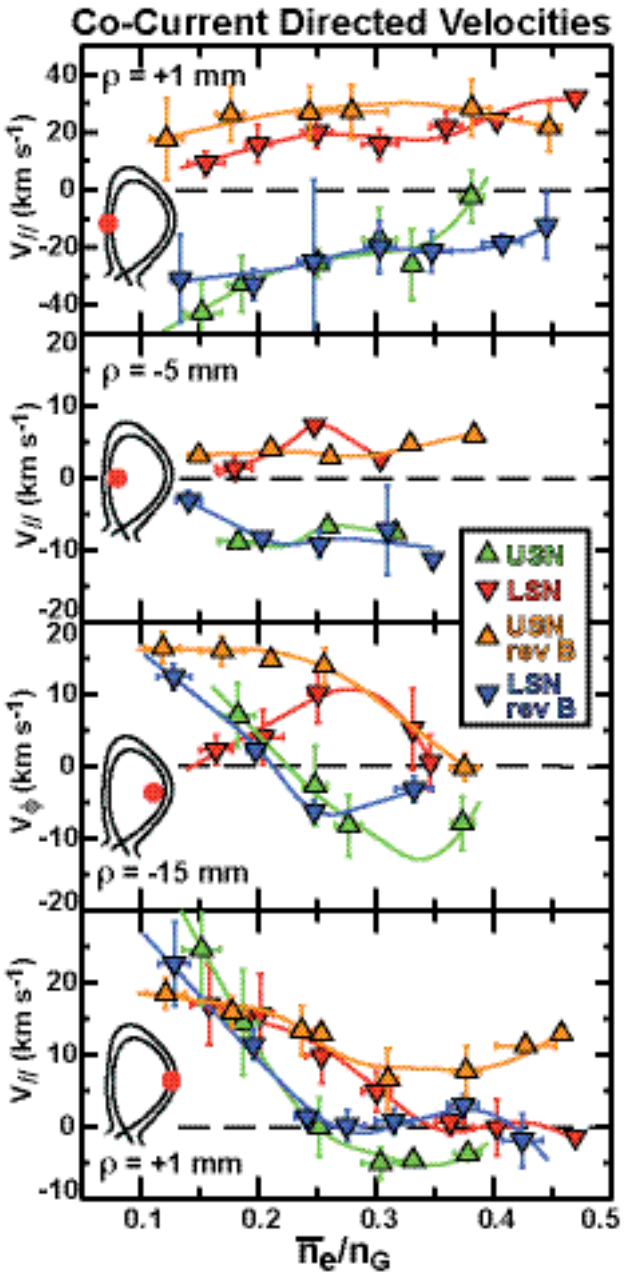

FIG. 9. (Color) Parallel ($V_{//}$) and toroidal (V_ϕ) flow velocities from Mach probes and CXRS diagnostics as a function of $\overline{n}_e / n_G$ for the four permutations of LSN/USN and normal/reversed fields. Positive values indicate a co-current directed flow. Measurement locations are listed (ρ values) as well as indicated on the inset graphics. Current and field magnitudes are the same as in Fig. 8: $I_p = 0.8$ MA, $B_T = 5.4$ tesla.

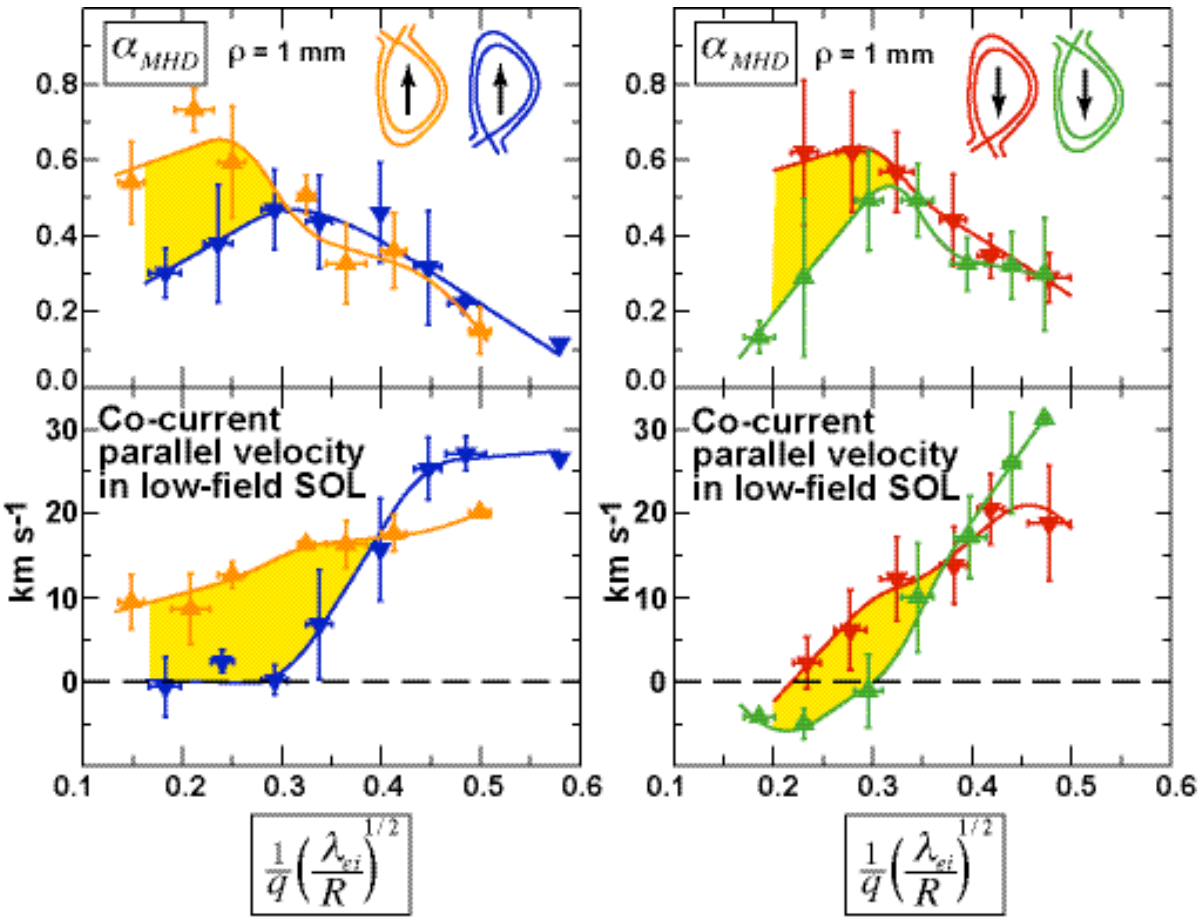

FIG. 10. (Color online) Normalized pressure gradients (α_{MHD}, top panels) and parallel flows in the low-field SOL (bottom panels) versus Λ, at a distance 1 mm outside the separatrix. Data are from matched LSN/USN discharges with reversed magnetic field (left panels) and forward magnetic field (right panels): $I_p = 0.8$ MA, $B_T = 5.4$ tesla, $0.12 < \bar{n}_e / n_G < 0.46$. For moderate to low values of Λ, the edge plasma attains significantly higher values of α_{MHD} with 'favorable $B \times \nabla B$', a condition that also produces co-current plasma rotation and enhanced co-current parallel flows in the low-field SOL (shaded regions).

References

[1] M. Greenwald, R. L. Boivin, F. Bombarda *et al.*, Nucl. Fusion **37**, 793 (1997).
[2] C. S. Pitcher, A. H. Boozer, H. Murmann, J. Sohweinzer, W. Suttrop, and H. Salzmann, Phys. Plasmas **4**, 2577 (1997).
[3] W. Suttrop, M. Kaufmann, H.J. de Blank *et al.*, Plasma Phys. Control. Fusion **39**, 2051 (1997).
[4] T.H. Osborne, R.J. Groebner, L.L. Lao, A.W. Leonard, R. Maingis, R.L. Miller, G.D. Porter, D.M. Thomas, and R.E. Waltz, Plasma Phys. Control. Fusion **40**, 845 (1998).
[5] J. W. Hughes, D. A. Mossessian, A. E. Hubbard, B. LaBombard, and E. S. Marmar, Phys. Plasmas **9**, 3019 (2002).
[6] M. Becoulet, G. Huysmans, Y. Sarazin *et al.*, Plasma Phys. Control. Fusion **45**, A93 (2003).
[7] A. E. Hubbard, R. L. Boivin, R. S. Granetz *et al.*, Phys. Plasmas **8**, 2033 (2001).
[8] C. M. Greenfield, K. H. Burrell, E. J. Doyle *et al.*, Plasma Phys. Control. Fusion **44**, A123 (2002).
[9] A. Loarte, B. Lipschultz, A. S. Kukushkin *et al.*, Nucl. Fusion **47**, S203 (2007).
[10] B. LaBombard, M. V. Umansky, R. L. Boivin, J. A. Goetz, J. Hughes, B. Lipschultz, D. Mossessian, C. S. Pitcher, and J. L. Terry, Nucl. Fusion **40**, 2041 (2000).
[11] B. LaBombard, R. L. Boivin, M. Greenwald, J. Hughes, B. Lipschultz, D. Mossessian, C. S. Pitcher, J. L. Terry, and S. J. Zweben, Phys. Plasmas **8**, 2107 (2001).
[12] M. Greenwald, Plasma Phys. Control. Fusion **44**, 27 (2002).
[13] B. LaBombard, J. E. Rice, A. E. Hubbard *et al.*, Nucl. Fusion **44**, 1047 (2004).
[14] B. LaBombard, J. E. Rice, A. E. Hubbard *et al.*, Phys. Plasmas **12**, 056111 (2005).
[15] B. A. Carreras, J. Nucl. Mater. **337-339**, 315 (2005).
[16] V. Naulin, J. Nucl. Mater. **363-365**, 24 (2007).
[17] B. D. Scott, Plasma Phys. Control. Fusion **49**, S25 (2007).
[18] B. Scott, Plasma Phys. Control. Fusion **39**, 1635 (1997).
[19] B. N. Rogers, J. F. Drake, and A. Zeiler, Phys. Rev. Lett. **81**, 4396 (1998).
[20] X. Q. Xu, R. H. Cohen, G. D. Porter, J. R. Myra, D. A. D'Ippolito, and R. Moyer, J. Nucl. Mater. **266**, 993 (1999).
[21] B. D. Scott, Phys. Plasmas **7**, 1845 (2000).
[22] B. D. Scott, Phys. Plasmas **12**, 102307 (2005).
[23] B. D. Scott, Plasma Phys. Control. Fusion **48**, A387 (2006).
[24] C. S. Chang and S. Ku, Contributions to Plasma Physics **46**, 496 (2006).
[25] X.Q. Xu and A.M. Dimits, Bull. Amer. Phys. Soc., CP8.00121 (2007).
[26] B. LaBombard, J.W. Hughes, D. Mossessian, M. Greenwald, B. Lipschultz, and J.L. Terry, Nucl. Fusion **45**, 1658 (2005).
[27] B. D. Scott, New Journal of Physics **4** (2002).
[28] A. Zeiler, D. Biskamp, J. F. Drake, and P. N. Guzdar, Phys. Plasmas **3**, 2951 (1996).
[29] B. N. Rogers and J. F. Drake, Phys. Rev. Lett. **79**, 229 (1997).
[30] J. W. Hughes, B. LaBombard, J. Terry, A. Hubbard, and B. Lipschultz, Nucl. Fusion **47**, 1057 (2007).
[31] C. Hidalgo, B. Goncalves, M.A. Pedrosa *et al.*, J. Nucl. Mater. **313-316**, 863 (2003).
[32] J. W. Connor, G. F. Counsell, S. K. Erents, S. J. Fielding, B. LaBombard, and K. Morel, Nucl. Fusion **39**, 169 (1999).

[33] G. F. Counsell, J. W. Connor, S. K. Erents, A. R. Field, S. J. Fielding, B. La Bombard, and K. M. Morel, J. Nucl. Mater. **266-269**, 91 (1999).
[34] K. McCormick, N. Asakura, S. Bosch *et al.*, J. Nucl. Mater. **266-269**, 99 (1999).
[35] J.W. Kim, D.P. Coster, J. Neuhauser, and R. Schneider, J. Nucl. Mater. **290-293**, 644 (2001).
[36] W. Suttrop, V. Mertens, H. Murmann, J. Neuhauser, and J. Schweinzer, J. Nucl. Mater. **266-269**, 118 (1999).
[37] J. Neuhauser, D. Coster, H.U. Fahrbach *et al.*, Plasma Phys. Control. Fusion **44**, 855 (2002).
[38] B. LaBombard, N. Smick, M. Greenwald, J.W. Hughes, B. Lipschultz, K. Marr, and J L Terry, Bull. Amer. Phys. Soc., JO1.00004 (2006).
[39] B. LaBombard, N. Smick, M. Greenwald, J. W. Hughes, B. Lipschultz, K. Marr, and J. L. Terry, J. Nucl. Mater. **363-365**, 517 (2007).
[40] I. H. Hutchinson, R. Boivin, F. Bombarda *et al.*, Phys. Plasmas **1**, 1511 (1994).
[41] J.W. Hughes, D.A. Mossessian, A.E. Hubbard, E.S. Marmar, D. Johnson, and D. Simon, Rev. Sci. Instrum. **72**, 1107 (2001).
[42] B. LaBombard, Phys. Plasmas **9**, 1300 (2002).
[43] N. Smick, B. LaBombard, and C.S. Pitcher, J. Nucl. Mater. **337-339**, 281 (2005).
[44] N. Smick and B. LaBombard, Bull. Amer. Phys. Soc., QP1.00066 (2006).
[45] R. McDermott, B Lipschultz, K. Marr, D. Whyte, and J W Hughes, Bull. Amer. Phys. Soc., NP8.00078 (2007).
[46] A. Graf, M. May, P. Beiersdorfer, D. Whyte, B. LaBombard, N. Smick, and K. Marr, Bull. Amer. Phys. Soc., NP8.00085 (2007).
[47] R. L. Boivin, J. A. Goetz, A. E. Hubbard *et al.*, Phys. Plasmas **7**, 1919 (2000).
[48] M. Greenwald, J. L. Terry, S. M. Wolfe, S. Ejima, M. G. Bell, S. M. Kaye, and G. H. Neilson, Nucl. Fusion **28**, 2199 (1988).
[49] J. L. Terry, S. J. Zweben, K. Hallatschek *et al.*, Phys. Plasmas **10**, 1739 (2003).
[50] B.A. Carreras, B. van Milligen, M.A. Pedrosa *et al.*, Phys. Rev. Lett. **80**, 4438 (1998).
[51] Y. Sarazin and Ph. Ghendrih, Phys. Plasmas **5**, 4214 (1998).
[52] B. A. Carreras, V. E. Lynch, and B. LaBombard, Phys. Plasmas **8**, 3702 (2001).
[53] S. I. Braginskii, "Transport Processes in a Plasma," in *Reviews of Plasma Physics* (Consultants Bureau, New York, 1965), Vol. 1, pp. 205.
[54] P. N. Guzdar, R. G. Kleva, P. K. Kaw, R. Singh, B. LaBombard, and M. Greenwald, Phys. Plasmas **14**, 020701 (2007).
[55] X.Q. Xu, W.M. Nevins, T.D. Rognlien, R.H. Bulmer, M. Greenwald, A. Mahdavi, L.D. Pearlstein, and P. Snyder, Phys. Plasmas **10**, 1773 (2003).
[56] X.Q. Xu, R.H. Cohen, W.M. Nevins *et al.*, "Density Effects on Tokamak Edge Turbulence and Transport with Magnetic X-points," in *Fusion Energy 2004* (Vienna: IAEA, 2004), Vol. CD ROM file TH/1-5 and http://www-naweb.iaea.org/napc/physics/fec/fec2004/datasets/index.html.
[57] B. D. Scott, Phys. Plasmas **12**, 062314 (2005).
[58] A. Kendl and B. D. Scott, Phys. Plasmas **13**, 012504 (2006).
[59] A. E. Hubbard, R. L. Boivin, J. F. Drake, M. Greenwald, Y. In, J. H. Irby, B. N. Rogers, and J. A. Snipes, Plasma Phys. Control. Fusion **40**, 689 (1998).

[60] F. Ryter, W. Suttrop, B. Brusehaber *et al.*, Plasma Phys. Control. Fusion **40**, 725 (1998).
[61] H. Biglari, P.H. Diamond, and P.W. Terry, Phys. Fluids. B. **2**, 1 (1990).
[62] R.J. Groebner, K.H. Burrell, and R.P. Seraydarian, Phys. Rev. Lett. **64**, 3015 (1990).
[63] K.H. Burrell, Phys. of Plasmas **4**, 1499 (1997).
[64] P.W. Terry, Rev. Mod. Phys. **72**, 109 (2000).
[65] J.W. Connor and H.R. Wilson, Plasma Phys. Control. Fusion **42**, 1 (2000).